Impact of Hydrodynamic Interactions on the Performance of a Three-float Multi-mode Wave Energy Converter M4 in Regular Waves

Liang Sun[1], Jun Zang[1], Peter Stansby[2], Efrain Carpintero Moreno[2], Paul H. Taylor[3], Rodney Eatock Taylor[3]
[1]WEIR Research Unit, Department of Architecture and Civil Engineering, University of Bath, UK
[2]School of Mechanical, Aerospace and Civil Engineering, University of Manchester, UK
[3]Department of Engineering Science, University of Oxford, UK
E-mail: *l.sun@bath.ac.uk, j.zang@bath.ac.uk, p.k.stansby@manchester.ac.uk, efrain.carpinteromoreno@manchester.ac.uk, paul.taylor@eng.ox.ac.uk, r.eatocktaylor@eng.ox.ac.uk*

Highlights:

- Numerical investigations of relative rotations and mean power captured by the three-float multi-mode wave energy converter M4 have been presented and discussed in the paper
- An increase of power of about three times is achieved at its peak value through optimisation of damping coefficient.
- Impact of hydrodynamic interactions on the performance of multiple M4 devices has been assessed by numerical model.

1. Introduction

The most challenging technical issue with wave energy conversion is how to design high performance wave energy devices with affordable costs. Researchers at the University of Manchester have developed a floating, three-body line absorber M4 (as shown in Fig.1) that can extract wave energy from various modes of relative motion (surge, heave and pitch) between the floating bodies [1, 2] and align with the wave directions automatically (only small angles between the horizontal longitudinal axis and mean wave directions are desirable). As a floating moored system, M4 is easily deployed and maintained compared with those systems consisting of fixed substructures. The single hinge for power take-off in M4 is accessible above the deck on "Float 2". By optimising the geometries of floats to minimise the energy loss due to viscous effects, up to 60% improvement of performance has been achieved [1, 2]. To give a better understanding of the hydrodynamic characteristics of M4 and assess the impact of hydrodynamic interactions on the performance, investigations have been made using a numerical tool based on the potential flow frequency domain code DIFFRACT [3].

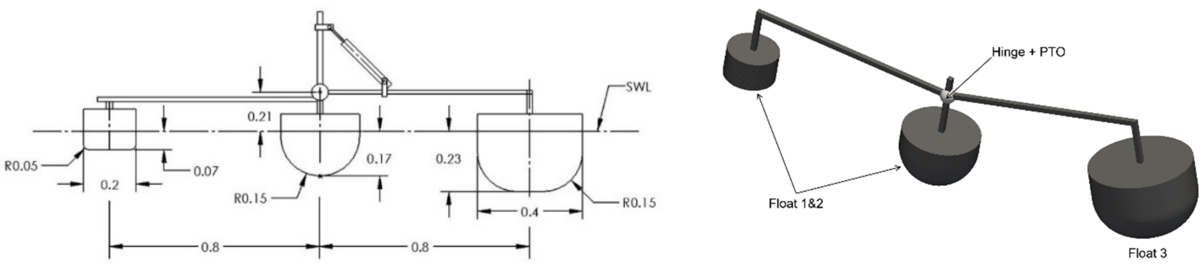

Fig.1 Laboratory-scaled model in wave basin (unit: m) and two-body dynamic system in numerical analysis

2. Multi-body Dynamic Model in Potential Flow Frame

Under the potential flow assumption, the motion equations for multiple floating bodies without mechanical connections can be written in the frequency domain [3]

$$\left[-\omega^2\left(\mathbf{M}+\mathbf{A}_H(\omega)\right)-\mathrm{i}\omega\left(\mathbf{B}+\mathbf{B}_H(\omega)\right)+\left(\mathbf{C}+\mathbf{C}_H\right)\right]\{\xi(\omega)\}=\{f_{ex}(\omega)\} \tag{1}$$

in which, vector $\{f_{ex}\}$ on the right hand side represents the linear wave excitation forces/moments which are related to the geometries of floating bodies and the incident waves (considering water depth d, wave height H, wave period T and wave direction β). The unknowns $\{\xi\}$ in Eq. (1) denote frequency dependent 6-degree motions of each floating body. The matrix $\mathbf{M}$ is the mass matrix for the N bodies, while $\mathbf{B}$ and $\mathbf{C}$ are external linear damping and stiffness matrices. Matrix $\mathbf{C}_H$ represents the hydrostatic and mooring restoring coefficients. Matrices $\mathbf{A}_H$ and $\mathbf{B}_H$ are the added mass and radiation damping matrices that are related to the radiation forces due to the body motions (determined by the geometries of bodies). Eq. (1) can be simplified as

$$[\mathbf{K}]\{\xi\}=\{f_{ex}\} \tag{2}$$

To consider the mechanical connections (e.g. hinges) between the floats in WECs, the technique of Lagrange multipliers $\{\lambda\}$ is introduced to define the generalized constraint forces and the motion equations become [3]

$$\begin{bmatrix}\mathbf{K} & \mathbf{D}^T\\ \mathbf{D} & 0\end{bmatrix}\begin{Bmatrix}\xi\\ \lambda\end{Bmatrix}=\begin{Bmatrix}f_{ex}\\ 0\end{Bmatrix} \tag{3}$$

where **D** is a constraint matrix, which defines the kinematic connectivity between the floating modules in the WECs. When PTOs are simplified as linear rotational dampers with damping coefficient B_d, the forces introduced by PTOs can be calculated using $f_{PTO}(\omega) = -B_d\dot{\theta}_r = i\omega B_d\theta_r$, where θ_r are relative rotations between the rigid modules. As shown in Fig.1, the bow float ("Float 1") and mid float ("Float 2") are rigidly connected by a beam, which can be modelled as a combined body and referred as "Float 1&2" in the present numerical analysis. Mass and inertia (about CoG) of the current two-body dynamic system have been listed in Table 1. The relative pitch motion at the hinge can be calculated as $\theta_r = \xi_{11} - \xi_5$. Here ξ_1 to ξ_6 denote 6 degrees of motions of "Float 1&2" and ξ_7 to ξ_{12} are for "Float 3" in the numerical model. The motion equations of interconnected multiple floats containing PTOs becomes

$$\begin{bmatrix} \mathbf{K} & \mathbf{D}^T \\ \mathbf{D} & 0 \end{bmatrix} \begin{Bmatrix} \xi \\ \lambda \end{Bmatrix} = \begin{Bmatrix} f_{ex} + f_{PTO} \\ 0 \end{Bmatrix} \tag{4}$$

The unknown θ_r can be moved to the left hand side of Eq. (4) and the corresponding coefficients can be absorbed into matrix **K**. The motion equations for WEC become

$$\begin{bmatrix} \mathbf{K}_2 & \mathbf{D}^T \\ \mathbf{D} & 0 \end{bmatrix} \begin{Bmatrix} \xi \\ \lambda \end{Bmatrix} = \begin{Bmatrix} f_{ex} \\ 0 \end{Bmatrix} \tag{5}$$

The mass and inertia of floats, damping moments of PTO, hydrostatic and radiation forces have been considered in matrix $\mathbf{K_2}$. There is no external damping and the effect of mooring forces is assumed to be small (**B**=0 and **C**=0).

The mean power captured by the WEC in regular waves at period T can be written as $P_c(T) = 2\pi^2 B_d |\theta_r|^2 / T^2$ [4]. To assess the performance of WEC in arrays, q-factor is usually used indicating the impact of hydrodynamic interactions on power absorption, which can be defined as $q = P_{c,array}(T) / N_{array} / P_{c,isolated}(T)$ [5]. Here N_{array} is the number of devices in the array. However, the q-factor is not sufficient to show the effects of multi-body interactions on the performance of WECs in arrays because it hides the real amount of absorbed power [4]. Here we use a modified factor q_{mod} to assess the performance of WECs in arrays, namely

$$q_{\text{mod}} = \frac{P_{c,array}(T) - N_{array} P_{c,isolated}(T)}{N_{array} \max\{P_{c,isolated}(T)\}} \tag{6}$$

where $\max\{P_{c,isolated}(T)\}$ is the maximum absorbed power across all periods experienced by an isolated WEC. If $q_{\text{mod}}<0$, the average power captured by each WEC in the array is less than the power from an isolated WEC, which indicates that wave interactions have a negative effect on the power absorption in arrays. Conversely, the park effect is regarded as constructive if $q_{\text{mod}}>0$.

3. Validation of Numerical Model

The experiments were carried out in the COAST wave basin at Plymouth University with water depth of 1.0m. The tests can be divided into 2 groups according to the wave heights ($H\approx0.03$m and $H\approx0.05$m) as shown in Table 2. Both wave heights H and mechanical damping of PTO B_d were different for wave periods of T=0.6-1.6s (ΔT=0.1s). Direct comparisons between measurements and numerical results have been made for relative rotations θ_r and mean power P_c as shown in Fig. 2 and Fig.3. It can be seen that the present linear model can provide satisfactory predictions. The largest relative rotation is about 10° when $H\approx0.05$m at T=1.2s and the corresponding mean power is 1.13W. Due to the variations of H and B_d as seen in Table 2, the values of θ_r in Fig.2 and Fig.3 are not following a linear relationship between the two nominal wave heights.

Table 1 Mass and inertia of physical model (about CoG)

	Float 1&2	Float 3
Mass (kg)	10.1	24.0
X_{CoG} (m)	-0.169	0.793
Y_{CoG} (m)	0.0	0.0
Z_{CoG} (m)	-0.071	-0.120
I_{xx} (kg m^2)	0.2682529	0.647939
I_{yy} (kg m^2)	1.3184478	0.686797
I_{zz} (kg m^2)	1.2052959	0.730414

Table 2 Wave heights H and B_d in experiments

	$H\approx0.03$m		$H\approx0.05$m	
T (s)	H (m)	B_d (Nms)	H (m)	B_d (Nms)
0.6	0.019746	6.61587	0.045397	8.94465
0.7	0.021470	9.77849	0.037759	6.42148
0.8	0.025940	4.41930	0.044075	4.56104
0.9	0.024580	6.40728	0.042011	3.88574
1.0	0.022978	6.66238	0.035913	3.78748
1.1	0.024031	5.63643	0.041114	3.28271
1.2	0.024798	5.65411	0.042456	3.03081
1.3	0.025617	6.76979	0.045188	4.11856
1.4	0.025019	8.08623	0.044787	6.11586
1.5	0.024414	9.57468	0.045329	7.59046
1.6	×	×	0.041957	8.77892

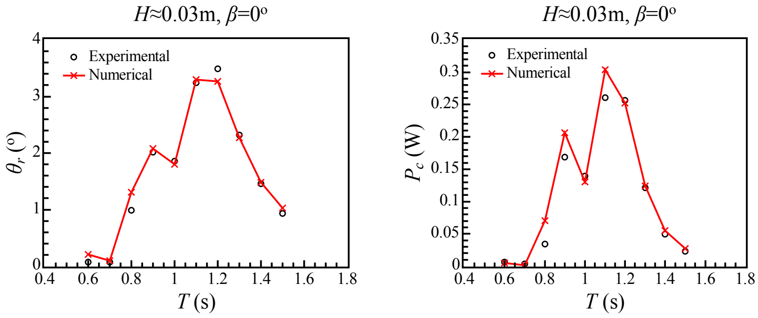

Fig.2 Measured and calculated relative rotation and mean power of M4 in regular waves (H≈0.03m)

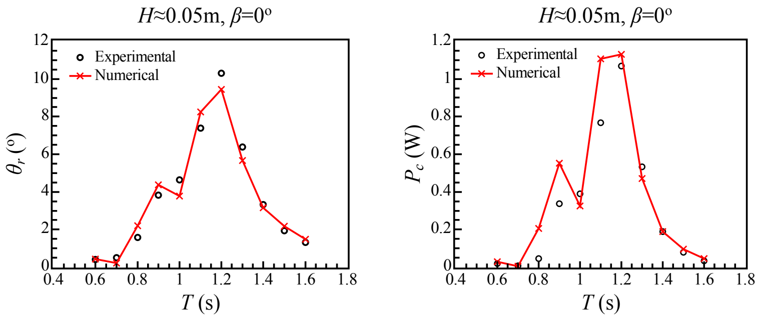

Fig.3 Measured and calculated relative rotation and mean power of M4 in regular waves (H≈0.05m)

4. Hydrodynamic Interactions between Floats of Single Device in Regular Waves

In the following numerical analysis, the wave height is set as H=0.03m where there is accurate prediction. After optimisation, B_d is chosen as 0.8Nms to get maximum power at the peak period (T=1.16s) in range of T=0.6-1.6s (ΔT=0.02s). As shown in Fig.1, M4 is a multi-body WEC which can only capture wave energy from the relative pitch motions about the hinge. It is important to assess the influence of roll and yaw motions when waves come from nonzero angle. Roll and yaw motions of M4 under different wave directions (β=5° and 10°) are shown in Fig.4. The largest roll and yaw motion are found at T=1.28s. The roll motion is up to 18° when β=10° (here we have not considered the additional roll damping due to the viscosity of the fluid). Maximum mean power is obtained at T=1.16s in Fig.4, which are $\max\{P_{c,isolated}(T)\}$ =0.985W for β=0°, $\max\{P_{c,isolated}(T)\}$ =0.974W for β=5°, $\max\{P_{c,isolated}(T)\}$ =0.943W for β=10°. Comparing with the mean power in experiments seen in Fig. 2, about three times of power is achieved at peak value through optimisation of the PTO. For a single device, the reductions of power due to the variations of wave directions in this range are negligible. Of course, the mean power captured by M4 may be affected, probably reduced, by the nonlinear buoyancy and excitation forces due to the large amplitude motions.

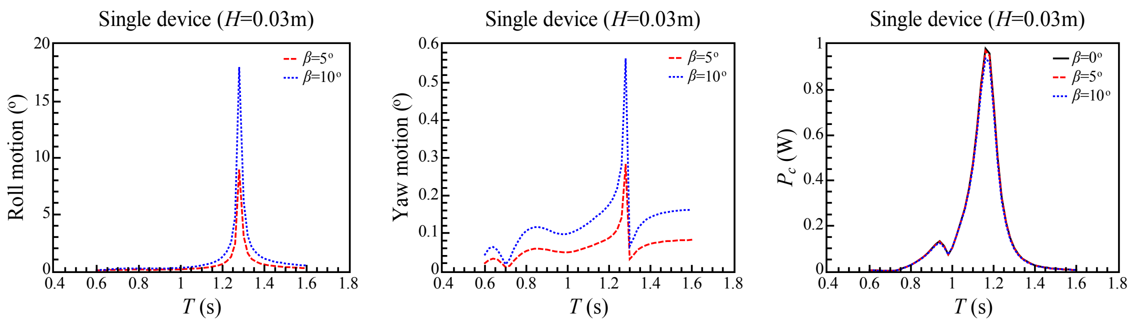

Fig.4 Rotational motions and mean power of single device under different wave directions

5. Hydrodynamic Interactions between Multiple Devices in Regular Waves

To understand the park effects in the arrays of M4, roll and yaw motions of each device are shown in Fig.5 for two devices in a side-by-side layout when β=0°. Three spacings (centres to centres of floats) are chosen, which are 1.0m, 2.0m and 4.0m. As expected, larger roll and yaw motions are found when spacing between two devices is smaller. Comparing with the results of roll and yaw motions in Fig.4, more peaks are found in short waves apart from the peaks at T=1.28s due to the existence of the second device. Mean power of each M4 in a two-device array is also compared with a single device. Reduction of peak value of mean power (-22% as shown in Fig. 5) is found when spacing=1.0m and more power (5% as shown in Fig.5) is obtained when spacing=2.0m. The influence of the second device is negligible at T=1.16s when spacing=4.0m.

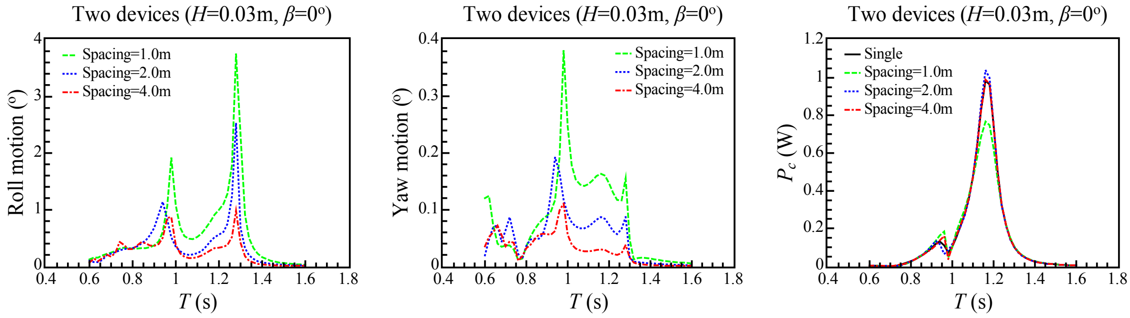

Fig.5 Rotational motions and mean power of each device in two-device array (β=0°)

To show park effect more directly, the modified q-factors (q_{mod} as defined in Eq. (6)) of different arrays in side-by-side layout (β=0°) are shown in Fig.6. It can be seen that constructive and destructive effect changes with wave period. Both constructive and destructive effect becomes more significant when more devices are in the arrays. When there are five devices, the modified q-factor is up to 0.13 (constructive effect) at T=0.96s when spacing=4.0m and down to -0.28 (destructive effect) at T=1.18s when spacing=1.0m. At peak period T=1.16s, destructive effect is found when spacing=1.0m. Constructive effect is found when spacing=2.0m and 4.0m, which is up to 9% of the peak value of mean power $\max\{P_{c,isolated}(T)\}$ in five-device array (spacing=2.0m).

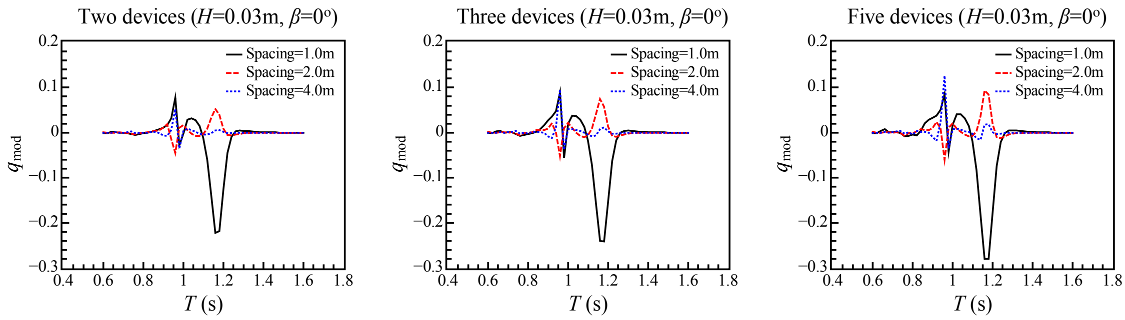

Fig.6 Modified q-factor of different arrays in side-by-side layout (β=0°)

6. Discussions

The limitations of linear potential flow models are well known. But they still offer a powerful numerical tool at the early stage of development of WECs. Comparisons of relative rotations and mean power in regular waves have confirmed that the three-float multi-mode WEC M4 can be represented as a linear dynamic system. An increase of power of about three times is achieved at its peak value through optimisation of the damping coefficient of the PTO. The spacings of devices in arrays of side-by-side layout have significant impact on the performance of M4. Further assessments of performance will be carried out for M4 in irregular waves considering different wave energy spectra, which will be discussed in the workshop.

Acknowledgements

This work was carried out within the Supergen Marine Challenge grant Step WEC (EP/K012487/1) which has been funded by the UK Engineering and Physical Sciences Research Council (EPSRC). Some of the analysis was performed on Bath HPC facility Balena.

References

[1] Stansby, P., Carpintero Moreno, E., Stallard, T., 2015. Capture width of the three-float multi-mode multi-resonance broad-band wave energy line absorber M4 from laboratory studies with irregular waves of different spectral shape and directional spread. Journal of Ocean Engineering and Marine Energy, Vol. 1, No.3, pp. 287-298.

[2] Stansby, P., Gu, H., Carpintero Moreno, E., Stallard, T. 2015. Drag minimisation for high capture width with three float wave energy converter M4. In: The 11th European Wave and Tidal Energy Conference (EWTEC 2015), 6-11 September, Nantes, France.

[3] Sun, L., Eatock Taylor, R., Choo, Y.S., 2012. Multi-body dynamic analysis of float-over installations. Ocean Engineering, Vol. 51, pp. 1-15.

[4] Babarit, A., 2010. Impact of long separating distances on the energy production of two interacting wave energy converters. Ocean Engineering, Vol. 37, pp. 718-729.

[5] Babarit, A., 2013. On the park effect in arrays of oscillating wave energy converters. Renewable Energy, vol. 58, pp. 68-78.